# Expanding the Toolbox: From High-End to Low-Cost in Permanent Laser Scanning Applications

**Daniel CZERWONKA-SCHRÖDER, Germany, Ute HOLTKAMP, Germany, Solveig SANDER, Germany and Yihui YANG, Germany**

**Key words**: Deformation measurement; Engineering survey; Laser scanning; Low-cost technology; Risk management

## SUMMARY

Permanent Laser Scanning (PLS) has become a valuable tool in Earth observation and environmental monitoring, enabling continuous 3D measurements of dynamic surface processes. High-end instruments such as RIEGL scanners deliver benchmark accuracy at the millimeter level, yet their high costs restrict widespread use beyond research projects. Low-cost LiDAR sensors, like the Livox Avia, offer a more affordable alternative and raise the question of how far they can complement established systems.

Within the BMFTR-funded research project AImon5.0, both sensor types were deployed under identical conditions at a monitored rockfall site in Trier. A controlled displacement experiment using a planar reference target was conducted to enable a quantitative comparison of both systems under well-defined conditions. The evaluation follows a plane-based processing workflow including point cloud registration, plane estimation, and displacement analysis. The paper presents the results of the controlled displacement experiment and analyses the displacement detection performance of a high-end and a low-cost LiDAR system under identical experimental conditions.

The contribution provides a detailed description of the experimental setup, the applied processing workflow, and the comparative findings. The accuracy of the displacement estimates is quantified using the mean absolute distance deviation as an external quality measure. This forms the basis for further discussion on the potential roles of different sensor classes in PLS-based Earth observation and environmental monitoring.

# Expanding the Toolbox: From High-End to Low-Cost in Permanent Laser Scanning Applications

**Daniel CZERWONKA-SCHRÖDER, Germany, Ute HOLTKAMP, Germany, Solveig SANDER, Germany and Yihui YANG, Germany**

## 1. INTRODUCTION

Permanent Laser Scanning (PLS) describes the repeated acquisition of terrestrial LiDAR point clouds from a fixed scanner position over extended periods of time. By explicitly incorporating time as a fourth dimension, PLS enables the observation and analysis of dynamic surface processes in four dimensions (3D + time), allowing not only the quantification of net changes between epochs but also the investigation of temporal patterns and process dynamics. PLS is now an established monitoring approach in geoscientific and environmental applications, including rockfall and landslide monitoring, glacier dynamics, coastal and fluvial morphodynamics, as well as vegetation and snow cover studies (Lindenbergh et al., 2025).

High-end terrestrial laser scanners currently represent the benchmark for PLS applications due to their high ranging accuracy, long measurement ranges, and robust system integration, enabling reliable long-term operation even under demanding environmental conditions. However, the high acquisition and operational costs of such systems limit scalability and often restrict permanent installations to a small number of high-priority sites or well-funded research projects (Czerwonka-Schröder et al., 2025).

In parallel to these developments, the availability of low-cost LiDAR sensors has increased rapidly in recent years. Driven primarily by advances in autonomous driving, robotics, and mobile mapping, these sensors are characterized by compact designs, reduced hardware costs, and increasing openness with respect to software integration. Systematic reviews of low-cost 3D mapping solutions emphasize that such sensors are gaining relevance in geospatial applications, while also stressing that the term "low-cost" is inherently relative and that sensor performance strongly depends on the intended application and operating conditions (Balado et al., 2025). Although promising results have been reported for episodic surveys and short-term or semi-permanent monitoring applications (e.g., Kelly et al., 2022; Perks et al., 2024; de Vugt et al., 2025; Geißendörfer & Holst, 2025; Výbošťok et al., 2025), the suitability of low-cost LiDAR sensors for permanent laser scanning remains an open research question. In contrast to episodic use cases, PLS requires long-term stability, predictable noise behavior under continuous operation, robustness against environmental influences, and reliable integration into automated processing workflows.

Within the BMFTR-funded research project AImon5.0, the opportunity arose to investigate this question under fully operational PLS conditions. At a permanently instrumented rockfall monitoring site near Trier (Germany), a low-cost LiDAR sensor (Livox Avia) was deployed in parallel with an established high-end permanent laser scanning system (RIEGL VZ-2000i) and operated under identical environmental conditions. This setup enables a direct, application-oriented comparison focused on the requirements of permanent operation.

The aim of this contribution is to assess whether low-cost LiDAR sensors can reliably complement high-end systems in PLS workflows. By analyzing displacement detection behavior, the paper provides an empirical evaluation of the potential and limitations of low-cost sensors for long-term PLS-based monitoring applications.

## 2. STUDY AREA AND DATASET

The investigation was carried out at the Trierer Augenscheiner, an unstable rock slope situated along the Mosel River at the northern edge of Trier in Rhineland-Palatinate, Germany. The slope is affected by gravitational mass movements and represents a direct hazard to nearby transport infrastructure. Due to its geological setting and documented activity, the site provides a realistic test environment for the application of PLS. The selection and instrumentation of the site were conducted within the framework of the research project AImon5.0 (Czerwonka-Schröder et al., 2025).

A permanent monitoring system was installed at the municipal swimming pool facilities, resulting in a typical observation distance of about 250–300 m between the sensors and the monitored slope. The main sensor is a RIEGL VZ-2000i terrestrial laser scanner, which is operated fully automatically. Standard scans are acquired once per hour with an angular resolution of 15 mdeg, while additional high-resolution scans with an angular resolution of 5 mdeg are performed at six-hour intervals. An overview of the permanent monitoring setup and the additional sensors deployed within the AImon5.0 project is shown in Czerwonka-Schröder et al. (2025).

In addition to the permanent installation, a dedicated measurement experiment was conducted on 8 January 2025 between 09:43 and 11:50 local time to evaluate the ability of a low-cost LiDAR sensor to detect small and controlled surface displacements. As natural rockfall activity at the Trierer Augenscheiner is neither temporally predictable nor controllable in magnitude, a reproducible experimental setup was required for a sensor comparison.

A planar target was mounted on a precise cross slide and positioned on a tripod in front of the rock slope. The cross slide allowed controlled in-plane displacements of up to 80 mm. Both the high-end terrestrial laser scanner and the low-cost LiDAR sensor simultaneously observed the same target while identical displacements were applied. The high-end scanner observed the target from the permanent monitoring position at approx. 250–300 m, whereas the low-cost sensor was installed at the foot of the slope at a significantly shorter range of approximately 60 m. The spatial configuration of the permanent PLS installation, the position of the low-cost sensor, and the experimental target is illustrated in Figure 1.

The measurement protocol consisted of three phases. First, both sensors recorded the static target over a period of one hour at three-minute intervals to assess short-term stability and temperature-related effects during sensor acclimatization. Second, 20 parallel acquisitions were performed, with the target incrementally displaced by 4 mm between consecutive scans, resulting in a total displacement of 80 mm. This phase served to evaluate the minimum detectable displacement for each sensor. Third, after reaching the final target position, both sensors acquired ten additional scans at two-minute intervals to analyze measurement behavior under static conditions.

Low-cost data acquisition was performed using a Livox Avia LiDAR sensor. The sensor was operated in a static configuration using the non-repetitive scanning mode, providing full field-of-view coverage and increasing point density with scan duration of 3000 ms. Frame time and acquisition intervals were configured according to a predefined measurement scheme, and raw point cloud data were recorded locally for each scan. In total, 50 parallel point clouds were acquired with each scanner during the experiment. The Livox Avia measurements were recorded synchronously with the RIEGL VZ-2000i data and form the dataset used for the comparative analyses presented in this contribution.

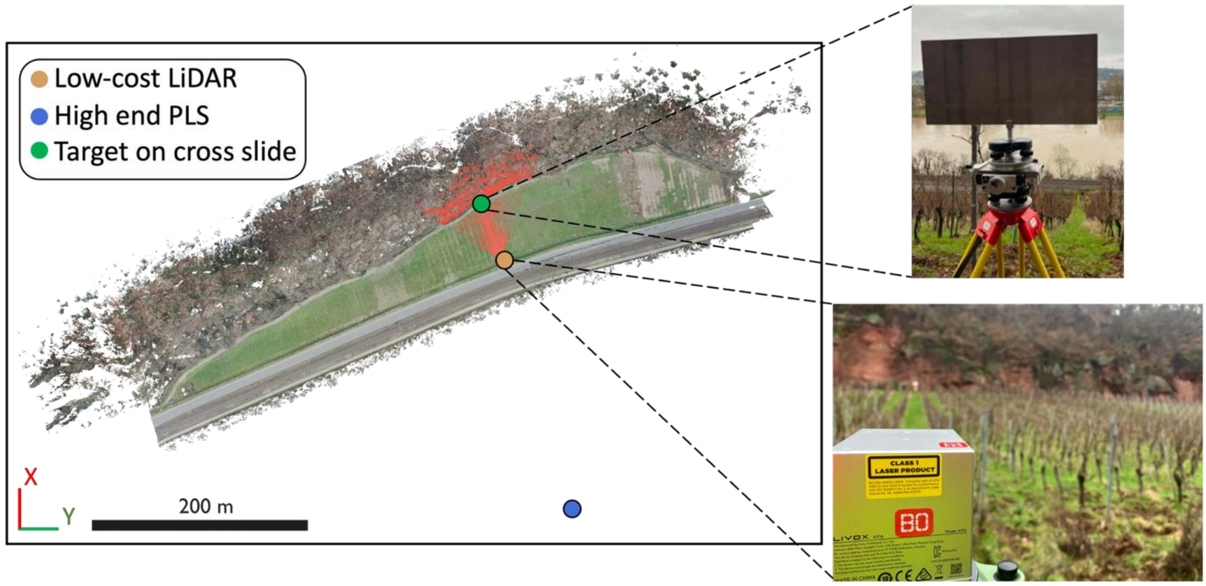


**Figure 1:** Sensor configuration at the Trierer Augenscheiner showing the high-end z zPLS installation, the low-cost LiDAR sensor, and the planar target used for the controlled displacement experiment.

## 3. METHODOLOGY

This section describes the workflow applied to analyze the experimental datasets acquired with the high-end and low-cost LiDAR systems. The methodology follows a structured evaluation chain commonly used in point cloud–based change analysis. The individual processing steps are designed to progressively reduce non-geometric effects and to isolate the controlled surface displacements introduced during the experiment.

First, the point cloud data are filtered, and registered to ensure that subsequent analyses are not influenced by sensor-related artefacts or setup instabilities (Sections 3.1 and 3.2). Based on the registered datasets, the planar target is then modelled for each acquisition epoch using plane adjustment (Section 3.3). Finally, the estimated planes are compared across time to derive displacement measures and sensor-specific quality metrics, which form the basis for the comparative evaluation (Section 3.4).

### 3.1 Point cloud filtering

Prior to further analysis, the acquired point cloud data were subjected to a filtering and cleaning procedure to remove vegetation and isolated measurements while preserving the geometric integrity of the planar target surface. All preprocessing steps were applied independently to the datasets of both sensor systems.

Filtering was performed using LAStools (rapidlasso, 2024), applying an iterative statistical outlier removal strategy. As the datasets do not contain information on first and last pulse returns, echo-based ground classification was not applicable. Vegetation and non-target elements were therefore treated as outliers and removed based on their local point density and spatial isolation.

Outlier removal was carried out using the lasnoise module in multiple successive passes. In each pass, points with a significantly reduced number of neighbors within a defined local neighborhood were classified as noise and removed. The filtering parameters were adjusted iteratively, with the output of each step serving as input for the subsequent one, allowing a gradual refinement of the point clouds.

A spatial thinning of the point clouds or restriction to a subregion using 3D bounding boxes was not required. The acquisition geometry and scanner configurations were defined in advance such that the recorded scene was largely limited to the target area. The resulting filtered point clouds contain only points representing continuous, stable surfaces and form the basis for the subsequent registration and surface modelling steps.

### 3.2 Point cloud registration

Following filtering, the temporal stability of the point cloud time series was assessed in order to distinguish sensor-related effects from actual surface displacements. The datasets acquired during the static phases of the experiment were analyzed to evaluate short-term stability and potential temperature-related influences.

To reduce residual misalignments between consecutive acquisitions, a registration step was applied within each sensor-specific point cloud time series, i.e., registration was performed independently for each sensor to avoid cross-sensor bias. A piecewise iterative closest point (Piecewise-ICP) approach was employed, which enables accurate registration of 4D data acquired by the PLS system based on automatically identified stable areas and is therefore robust against unexpected outliers and deformations during the monitoring period (Yang & Holst, 2025).

As an extension of robust bi-temporal point cloud registration (Yang & Schwieger, 2023), Piecewise-ICP takes multi-temporal point clouds as input and organizes them according to their associated temporal information. The 4D data registration process is then decomposed into multiple pairwise registrations, where the pair sequence is determined by means of the approximate overlap ratio for each potential pairing. Assuming minimal movement of the PLS platform during the monitoring period, all scans are regarded as coarsely pre-aligned. Therefore, fine registration is directly conducted for each determined pair of point clouds using an efficient and robust method based on a planar patch-based segmentation strategy, yielding transformation parameters, including rotation and translation, for each pairwise registration. By defining a reference epoch (e.g., the first epoch) and applying the derived pairing sequence, the final transformation of each point cloud with respect to the reference scan is subsequently computed. Further methodological details can be found in Yang and Holst (2025).

Table 1 shows the selected key parameters used in Piecewise-ICP. The basic resolution and patch size represent the average point spacing and the approximate size of generated planar patches, respectively. The initial and the minimum distance threshold (DT) define the descending scheme for the DT used to distinguish between stable and unstable patches. Compared to high-end scanners, low-cost LiDAR sensors typically produce point clouds with lower spatial resolution and higher noise levels. Therefore, when processing Livox data, a higher basic point spacing and larger initial and minimum distance thresholds are adopted.

The outputs of Piecewise-ICP are time series of transformation parameters for all scans relative to the reference scan, which can be used in subsequent analyses of scanner stability and the effects of atmospheric refraction on the laser signals.

**Table 1:** Parameter settings for registering 4D data from two sensors using Piecewise-ICP.

| Sensor type | Basic resolution | Patch size | Initial DT | Minimum DT |
|---|---|---|---|---|
| RIEGL | 0.1 m | 1.5 m | 0.1 m | 0.03 m |
| Livox | 0.2 m | 1.5 m | 0.2 m | 0.05 m |

### 3.3 Plane adjustment

The estimation of planar surfaces is performed independently for each epoch and for each sensor dataset. In a first step, each point cloud is spatially restricted to the region that best represents the planar reference surface. This clipping is performed using interactive clipping tools in CloudCompare (2025) to define the reference geometry. For the processing of the full time series, the clipping procedure is applied consistently to all epochs using batch processing, ensuring an identical spatial extent for all subsequent analyses. As a result, one clipped point cloud is available for each epoch and for each sensor.

In the next step, planar surfaces are estimated for each epoch based on the clipped point clouds. Plane estimation is carried out using a least-squares adjustment formulated according to the Gauss–Helmert model. To improve numerical stability, a centroid reduction of the coordinates is applied prior to the adjustment. For each sensor, the centroid of the clipped point cloud in the reference epoch is computed. This centroid is subsequently subtracted from the original coordinates of all points in every epoch, ensuring that all epochs remain expressed in a consistent local coordinate system.

The plane is represented using the Hessian normal form. The plane is defined by a normal vector $\boldsymbol{n}$ and its orthogonal distance $\boldsymbol{d}$ to the origin. For a given point $\mathbf{P}_{\boldsymbol{i}}$ on the plane, the shortest distance to the origin is obtained by projecting the point onto the normalized normal vector $\mathbf{n}_{\mathbf{0}}$:

$$d = \frac{\mathbf{n} \cdot \mathbf{P}_i}{\| \mathbf{n} \|} = \mathbf{n}_0 \cdot \mathbf{P}_i \tag{1}$$

This formulation is used to establish one observation equation per point of the clipped point cloud. All points therefore contribute jointly to the estimation of the unknown plane parameters $\boldsymbol{n_x}, \boldsymbol{n_y}, \boldsymbol{n_z}$ and $\boldsymbol{d}$.

As the plane equation can be multiplied by an arbitrary non-zero scalar without changing the represented geometry, the resulting normal equation system is inherently singular. To resolve this ambiguity, a constraint is introduced requiring the normal vector to be of unit length:

$$\| \mathbf{n} \| = \sqrt{n_x^2 + n_y^2 + n_z^2} = 1 \tag{2}$$

With this constraint, the plane is uniquely defined by the normalized normal vector $\mathbf{n}_{\mathbf{0}}$ and the distance $\boldsymbol{d}$ to the origin.

Using the estimated plane parameters, the orthogonal projection of the origin onto the plane can be computed for each epoch. This projected point serves as a consistent geometric reference and is subsequently used for the comparison of planes between epochs and for the derivation of displacement-related quality metrics.

The described plane estimation procedure is applied independently to each epoch of the time series for both the high-end and the low-cost LiDAR datasets.

### 3.4 Quality metrics and comparative evaluation

Based on the plane estimation described in Section 3.3, an orthogonal projection of the origin onto each estimated plane is computed for every acquisition epoch. This projected point provides a unique and consistent geometric reference and enables a direct comparison of plane positions over time. Surface displacements are quantified along the plane normal direction using this reference.

Let $\mathbf{p}$ and $\mathbf{q}$ denote the orthogonal projections of the origin onto the estimated planes of two different epochs, respectively. The displacement measure $\boldsymbol{c}$ between the two planes is defined as the absolute projection of the vector difference onto the normalized plane normal vector $\mathbf{n_0}$:

$$c = | (\mathbf{q} - \mathbf{p}) \cdot \mathbf{n}_0 | \tag{3}$$

The scalar value $\boldsymbol{c}$ represents the displacement magnitude between two planes along the normal direction. Variations of $\boldsymbol{c}$ during static phases of the experiment are interpreted as sensor-related noise and residual instability, whereas systematic changes during the displacement phase reflect the applied surface translations.

For the assessment of external accuracy, the estimated displacements are compared to the known reference displacement applied during the experiment. Following Neitzel et al. (2010), the mean absolute distance deviation $\boldsymbol{R_E}$ is introduced as a quality measure:

$$R_E = \frac{1}{n} \sum_{i=1}^{n} | c_i - \tilde{c} | \tag{4}$$

where $\boldsymbol{n}$ denotes the number of evaluated displacement estimates, $\boldsymbol{c_i}$ the displacement derived from the plane comparison for epoch $\boldsymbol{i}$, and $\tilde{\boldsymbol{c}}$ the known reference displacement. The mean absolute distance deviation $\boldsymbol{R_E}$ corresponds to the mean absolute error of the plane-based displacement estimates with respect to the known reference displacement. The metric $\boldsymbol{R_E}$ directly answers the question of how large the mean absolute deviation from the known reference displacement is. It is used to evaluate the external accuracy of the plane-based displacement estimation for both sensor systems.

# 4. RESULTS

## 4.1 Point cloud registration

Figure 2 shows the point clouds of the observed target area after applying the Piecewise-ICP registration. Stable regions are highlighted in green, while areas classified as unstable are shown in red. Figure 2(a) corresponds to the low-cost LiDAR sensor (Livox), whereas Figure 2(b) shows the results for the high-end terrestrial laser scanner (RIEGL).

For both sensor systems, a sufficient number of stable regions are detected. In the Livox datasets, approximately 17% of the points are classified as stable in each epoch, while for the RIEGL datasets this proportion is approximately 30%. The difference is primarily attributed to the differing spatial resolution and data quality of the two systems. In both cases, the stable regions are spatially distributed across the observed surface, providing sufficient correspondences for the estimation of the registration parameters.

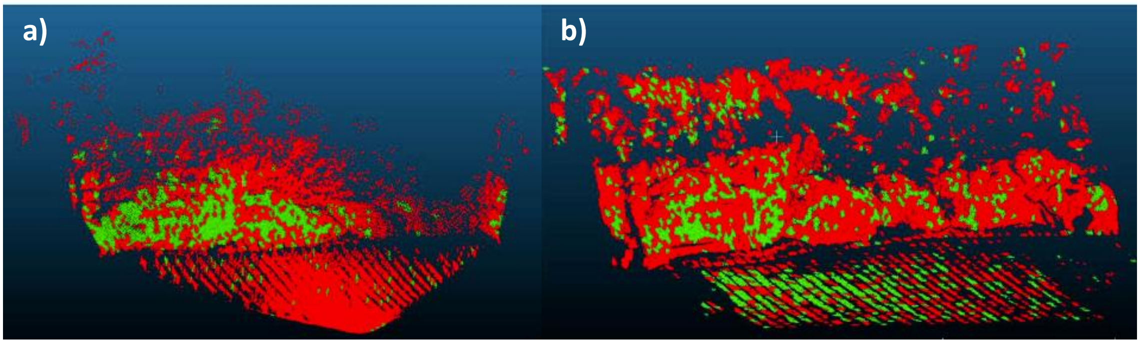


**Figure 2:** Spatial distribution of stable (green) and unstable (red) regions identified by Piecewise-ICP registration method. (a) Results for the Livox. (b) Results for the RIEGL.

Figure 3 presents the estimated transformation parameters for the RIEGL system over the duration of the experiment. The rotational parameters are shown in the upper panel, while the translational parameters are shown in the lower panel. All parameters fluctuate around zero without exhibiting systematic trends or offsets. This behavior indicates a consistent and stable acquisition geometry throughout the entire observation period.

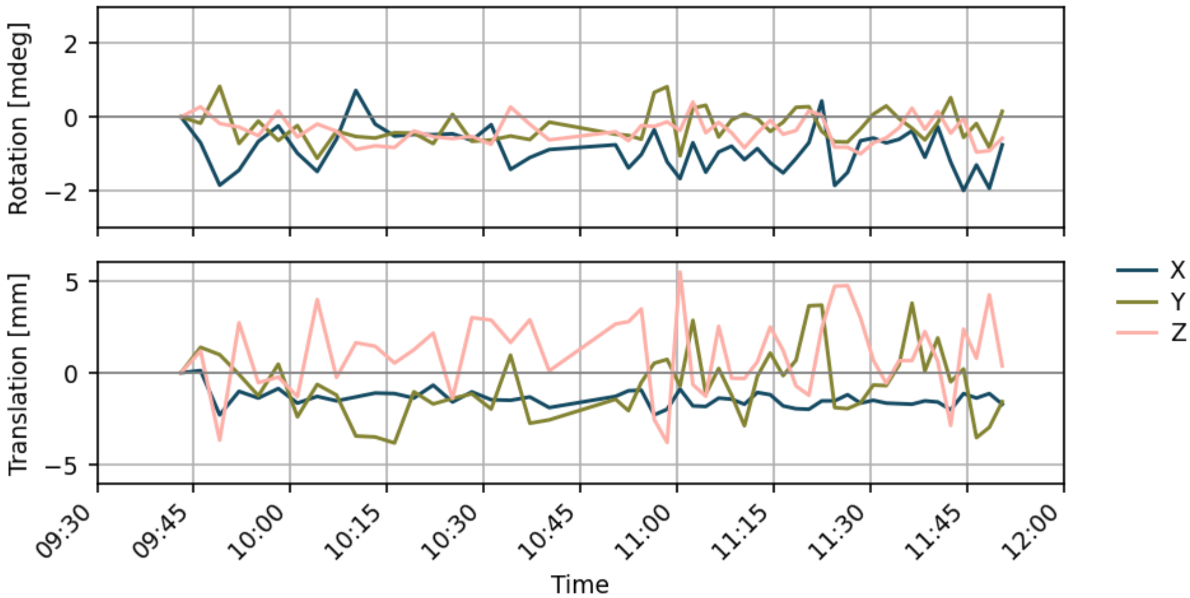


**Figure 3:** Estimated transformation parameters obtained from the registration of consecutive point clouds for the RIEGL system. Rotational parameters are shown in the upper panel and translational parameters in the lower panel.

The corresponding transformation parameters for the Livox system are shown in Figure 4. The overall behavior is analogous to that observed for the RIEGL system. The rotational parameters exhibit increased noise levels, approximately a factor of 2 to 5 higher than those of the RIEGL system, while no systematic deviations are observed. The translational parameters are of comparable magnitude for both systems. The increased variability of the rotational parameters is attributed to the lower spatial resolution and data quality of the Livox measurements.

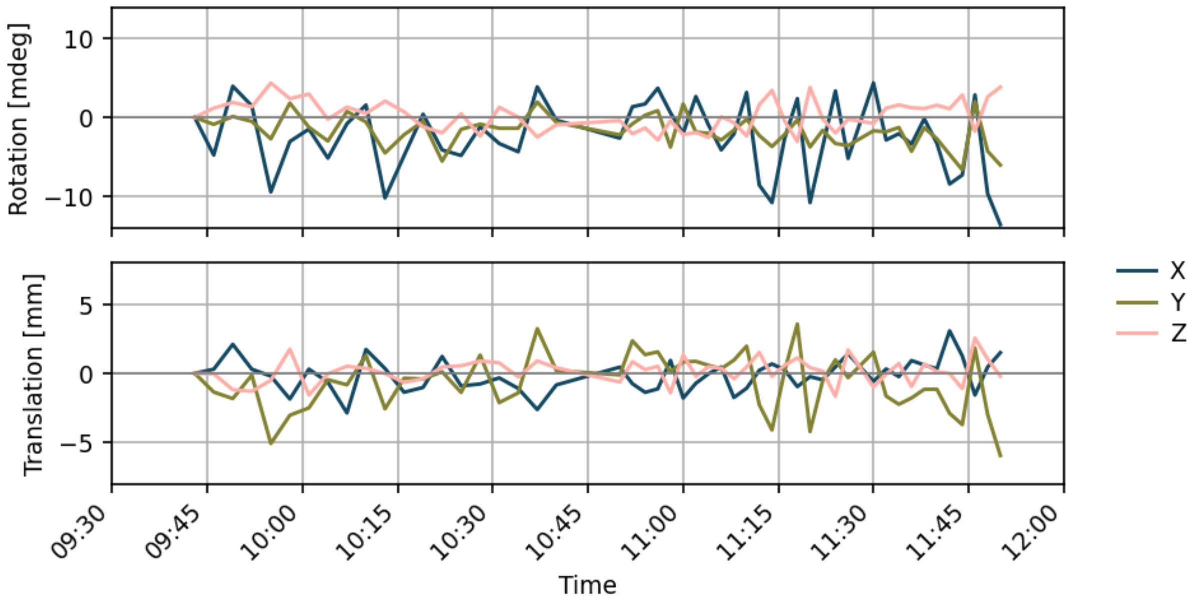


**Figure 4:** Estimated transformation parameters obtained from the registration of consecutive point clouds for the Livox sensor. Rotational parameters are shown in the upper panel and translational parameters in the lower panel.

Overall, the results demonstrate that the applied registration approach provides reliable and consistent results for both high-end and low-cost LiDAR data. Furthermore, the stability of the estimated transformation parameters confirms that a stable acquisition geometry prevailed throughout the experiment. Consequently, subsequent analyses can focus on actual surface displacements of the planar target, while other geometric influences can be largely excluded.

### 4.2 Displacement analysis

The results of the displacement analysis described in Section 3 are illustrated in Figure 5. The figure shows the time series of the displacement measure $\boldsymbol{c}$ for both sensor systems, with the RIEGL results shown in yellow and the Livox results shown in orange. The applied displacement of the reference plane is indicated in blue.

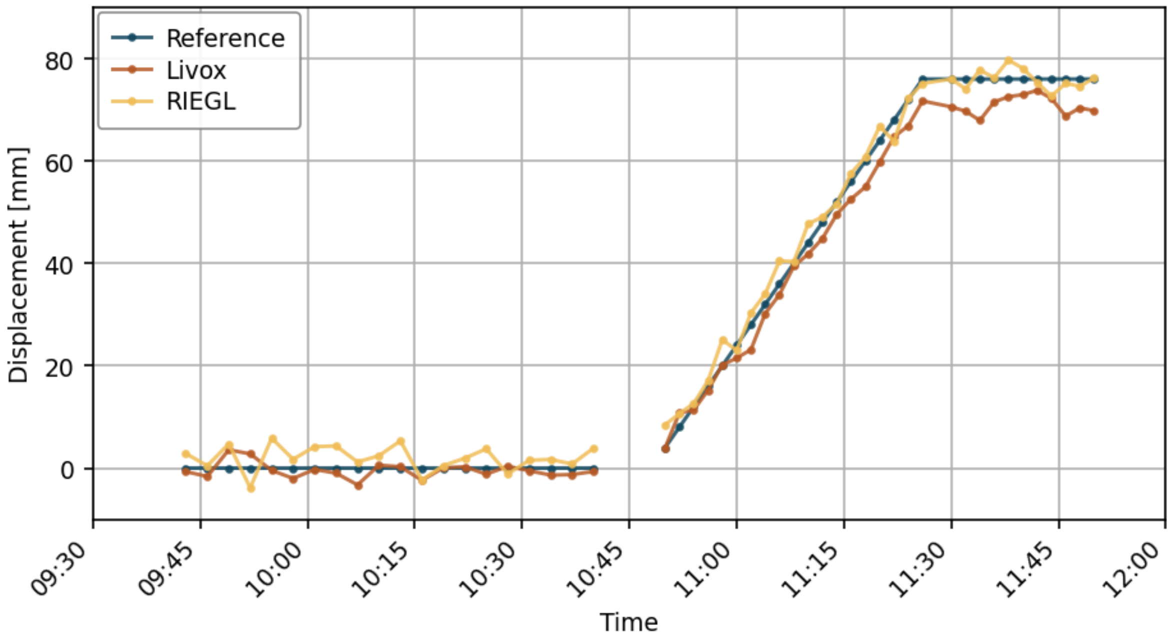


**Figure 5:** Time series of the plane-based displacement measure $\boldsymbol{c}$ during the controlled displacement experiment. The data gap between 10:40 and 10:50 represents a scheduled pause separating the initial static phase from the subsequent displacement phase, while the sensor systems remained powered on.

During the initial warm-up phase of approximately one hour (09:43 to 10:40), no systematic changes in the displacement measure are observed for either sensor system. In this phase, both time series exhibit normally distributed deviations around zero. The measurement noise of the RIEGL system is slightly higher than that of the Livox system during this period. At the end of the warm-up phase, no evidence of drift effects or other systematic influences related to sensor stabilization can be identified for either system.

Subsequently, the displacement behavior of the RIEGL system is analyzed in detail. Between 10:50 and 11:26, the planar target is incrementally shifted by 4 mm every two minutes towards the rock face, resulting in an increasing sensor-to-target distance for both systems. Over this entire displacement phase, as well as during the subsequent static phase from 11:30 to 11:50, the RIEGL time series shows normally distributed deviations around the expected displacement values. No indications of systematic deviations or gross errors are observed in the measurement series. According to Equation (4), the resulting mean absolute distance deviation for the RIEGL system is $\boldsymbol{R_E = 2.2}$ **mm**. The observed deviations are within the expected range specified by the manufacturer.

When analyzing the corresponding displacement phase for the Livox system, a different behavior is observed. From approximately 11:00 onwards, a systematic deviation towards negative values becomes apparent in the displacement time series. This behavior persists into the final static phase, during which systematic deviations in the range of approximately

3 to 7 mm are observed. The mean absolute distance deviation for the Livox system, computed according to Equation (4), is $\boldsymbol{R_E} = \mathbf{2.6\ mm}$. Despite the observed systematic deviation, this result indicates that low-cost LiDAR sensors exhibit potential for application within permanent laser scanning workflows.

However, the presence of a systematic deviation in the Livox data cannot be explained conclusively at this stage. Several potential influencing factors were examined. Instability of the experimental setup can be largely excluded due to the use of robust Piecewise-ICP registration. Unmodelled atmospheric effects are considered unlikely, as the maximum temperature variation during the experiment was limited to approximately 1.5 °C and the measurements were conducted under uniformly overcast conditions, minimizing solar radiation effects. A remaining potential cause is the missing or unknown calibration of the low-cost sensor and the temporal stability of its internal components, which has not yet been investigated further.

In line with the findings of Kelly et al. (2022), further investigations are required to characterize and understand such systematic effects in low-cost LiDAR sensors before their long-term deployment in permanent laser scanning applications.

## 5. CONCLUSION AND OUTLOOK

This paper investigated the applicability of a low-cost LiDAR sensor for permanent laser scanning using a controlled displacement experiment at a real-world monitoring site, with a high-end terrestrial laser scanner as reference. The evaluation followed a consistent processing chain comprising point cloud registration, plane-based displacement analysis, and accuracy assessment using the mean absolute distance deviation.

The results demonstrate that the applied Piecewise-ICP registration approach provides stable and consistent alignment for both sensor systems. The high-end system detects the imposed incremental displacements without systematic effects and within the expected accuracy range. The low-cost LiDAR sensor resolves the applied displacements at the millimeter level but exhibits a systematic deviation during the experiment, indicating sensor-specific influences that are not yet fully understood.

Despite this limitation, the findings show that low-cost LiDAR sensors have clear potential for displacement detection in PLS-related applications. Further investigations are required to analyze the influence of scan geometry, incidence angle, point density distribution, sensor calibration, and temporal stability, particularly with respect to long-term operation and varying environmental conditions.

If these systematic effects can be better characterized and mitigated, low-cost LiDAR sensors could become a technically viable and economically attractive option for permanent laser scanning. This would enable the deployment of dense monitoring networks and support large-scale, cost-efficient monitoring applications worldwide, which are of relevance to the geodetic community.

## REFERENCES


Balado, J., Garozzo, R., Winiwarter, L., & Tilon, S. (2025). A systematic literature review of low-cost 3D mapping solutions. Information Fusion, 114, 102656. https://doi.org/10.1016/j.inffus.2024.102656

CloudCompare (2025). CloudCompare – 3D point cloud and mesh processing software Open Source Project (Version 2.14.beta). https://www.cloudcompare.org/

Czerwonka-Schröder, D., Schulte, F., Albert, J., Höfle, B., Holst, C., & Zimmermann, K. (2025). AImon5.0 – Real-time monitoring of gravitational mass movements and critical infrastructure risk management with AI-assisted 3D metrology. In Proc. of the 6th Joint International Symposium on Deformation Monitoring (JISDM), Karlsruhe.

de Vugt, L., Carraro, E., Fatihi, A., Mattea, E., Myall, E., Czerwonka-Schröder, D., & Anders, K. (2025). Permanent laser scanning and 3D time series analysis for geomorphic monitoring using low-cost sensors and open-source software. The International Archives of the Photogrammetry, Remote Sensing and Spatial Information Sciences, XLVIII-G-2025, 359–365. https://doi.org/10.5194/isprs-archives-XLVIII-G-2025-359-2025

Geißendörfer, O., & Holst, C. (2025). Spatio-temporal mode description in LiDAR point clouds. In 6th Joint International Symposium on Deformation Monitoring (JISDM). Karlsruher Institut für Technologie (KIT). https://doi.org/10.5445/IR/1000180525

Kelly, C., Wilkinson, B., Abd-Elrahman, A., Cordero, O., & Lassiter, H. A. (2022). Accuracy Assessment of Low-Cost Lidar Scanners: An Analysis of the Velodyne HDL–32E and Livox Mid–40's Temporal Stability. *Remote Sensing*, *14*(17), 4220. https://doi.org/10.3390/rs14174220

Lindenbergh, R., Anders, K., Campos, M., Czerwonka-Schröder, D., Höfle, B., Kuschnerus, M., Puttonen, E., Prinz, R., Rutzinger, M., Voordendag, A., & Vos, S. (2025). Permanent terrestrial laser scanning for near-continuous environmental observations: Systems, methods, challenges and applications. ISPRS Open Journal of Photogrammetry and Remote Sensing, 17, 100094. https://doi.org/10.1016/j.ophoto.2025.100094

Neitzel, F., Mordwinzew, W., & Lerche, C. (2010). Untersuchung von Registrierungsverfahren hinsichtlich des Einsatzes terrestrischer Laserscanner in der Deformationsmessung. Allgemeine Vermessungs-Nachrichten (AVN), 6/2010, 213–218.

Perks, M. T., Pitman, S. J., Bainbridge, R., Díaz-Moreno, A., & Dunning, S. A. (2024). An evaluation of low-cost terrestrial LiDAR sensors for assessing hydrogeomorphic change. Earth and Space Science, 11(8), e2024EA003514. https://doi.org/10.1029/2024EA003514

rapidlasso. (2024). LAStools (Version 240416). https://rapidlasso.de/

Výbošťok, J., Chudá, J., Tomčík, D., Gretch, D., Tomaštík, J., Pełka, M., Będkowski, J., & Mokroš, M. (2025). An open and low-cost terrestrial laser scanner prototype: Delivering reliable accuracy for forest practice on a budget. SSRN. https://doi.org/10.2139/ssrn.5386703

Yang, Y., & Holst, C. (2025). Piecewise-ICP: Efficient and robust registration for 4D point clouds in permanent laser scanning. ISPRS Journal of Photogrammetry and Remote Sensing, 227, 481–500. https://doi.org/10.1016/j.isprsjprs.2025.06.026

Yang, Y., & Schwieger, V. (2023). Supervoxel-based targetless registration and identification of stable areas for deformed point clouds. Journal of Applied Geodesy, 17(2), 161–170. https://doi.org/10.1515/jag-2022-0031

## FUNDING

The BMFTR (Federal Ministry of Research, Technology and Space) is funding the joint project AImon5.0 within the funding measure ‘Digital GreenTech—Environmental Engineering meets Digitalisation’ as part of the ‘Research for Sustainability’ (FONA) Strategy under the funding code 02WDG1696.

## BIOGRAPHICAL NOTES

**Daniel Czerwonka-Schröder** received his PhD from TU Bergakademie Freiberg with a focus on Geomonitoring. He studied Surveying and Geoinformatics at Mainz University of Applied Sciences and previously worked at DMT GmbH & Co. KG on international multisensor monitoring projects integrating LiDAR, GNSS, and environmental sensors. His research focuses on PLS-based automated 4D geomonitoring and the integration of geodetic sensors into continuous monitoring workflows. He is Professor of Applied Geodesy and Geomonitoring at Bochum University of Applied Sciences and Head of the Laboratory for Geomonitoring and Sensor Integration, established in 2026, and a member of the DVW Working Group 8 (Mobile and Autonomous Sensor Systems) in Germany.

**Ute Holtkamp and Solveig Sander** completed their Bachelor’s degrees in Surveying at Bochum University of Applied Sciences in 2026 and 2025, respectively. During their studies, they contributed to student research projects focusing on the analysis and evaluation of terrestrial laser scanning and low-cost LiDAR data. Their work supported the processing, methodological development, and interpretation of the experimental results presented in this study.

**Yihui Yang** received his Ph.D. degree from University of Stuttgart with focuses on laser scanning-based deformation monitoring and point cloud registration. He obtained his B.Sc. and M.Sc. degrees in Geodesy and Geoinformatics in 2016 and 2019, respectively. From May to June 2023, he was a visiting researcher at Heidelberg University. He is currently an academic advisor at the Chair of Engineering Geodesy, Technical University of Munich, where his research interests include efficient LiDAR data processing, uncertainty analysis and reduction, and high spatiotemporal-resolution deformation analysis.

**CONTACT**

Prof. Dr.-Ing. Daniel CZERWONKA-SCHRÖDER
Bochum University of Applied Sciences
Am Hochschulcampus 1
44801 Bochum
GERMANY
Tel. +49 234 36186 -9713
Email: daniel.czerwonka-schroeder@hs-bochum.de
Web site: https://www.hochschule-bochum.de/fbg/team-und-labore/czerwonka-schroeder/